

## Phonon dispersion curves in dilute KTN crystals

This article has been downloaded from IOPscience. Please scroll down to see the full text article.

1996 J. Phys.: Condens. Matter 8 1135

(<http://iopscience.iop.org/0953-8984/8/9/006>)

View [the table of contents for this issue](#), or go to the [journal homepage](#) for more

Download details:

IP Address: 171.66.16.208

The article was downloaded on 13/05/2010 at 16:18

Please note that [terms and conditions apply](#).

## Phonon dispersion curves in dilute KTN crystals

L Foussadier†, M D Fontana† and W Kress‡

† Laboratoire Matériaux Optiques à Propriétés Spécifiques, CLOES, University of Metz and Supelec, 2 rue E Belin, 57078 Metz Cédex 3, France

‡ Max-Planck-Institut für Festkörperforschung, Postfach 800 665, D-70506 Stuttgart, Germany

Received 18 April 1995, in final form 12 October 1995

**Abstract.** The phonon dispersion curves of the transverse acoustic (TA) and the lowest transverse optic (TO) branches in the (001) direction of two  $\text{KTa}_{1-x}\text{Nb}_x\text{O}_3$  (KTN) crystals with niobium concentrations of 0.8 and 1.2 at.% have been measured by inelastic neutron scattering at various temperatures. A pronounced temperature dependence has been observed for both the lowest TO phonon at the centre of the Brillouin zone and the TA phonons in the (001) direction for reduced wave vectors larger than 0.04. The temperature dependence of the TA phonons at large wavevectors shows a significant minimum. From the observation of this minimum it is conjectured that both crystals undergo phase transitions.

The measured data have been analysed in the framework of a shell model with an anisotropic, nonlinear core–shell interaction. It is shown that the anomalous behaviour of the TA branch is due to an exchange of vibrational character between the phonons of the lowest TO branch and those of the TA branch. An estimate of the size of dipolar clusters around the niobium impurities is derived from the analysis of the dispersion of the lowest TO modes in the long-wavelength range.

### 1. Introduction

Solid solutions of  $\text{KTa}_{1-x}\text{Nb}_x\text{O}_3$  (KTN) have attracted considerable interest during recent years since they provide a model system for the study of effects of impurities on phase transitions.

Pure  $\text{KTaO}_3$  is an incipient ferroelectric. It shows the characteristic of a ferroelectric in the paraelectric phase but does not undergo any phase transition and remains cubic down to temperatures of 0 K. The lowest transverse optic (TO) phonon of  $\text{KTaO}_3$  starts to soften with decreasing temperature as in a ferroelectric. As  $T = 0$  K is approached quantum fluctuations become important and lead to characteristic deviations from a Curie–Weiss law. These quantum fluctuations finally stabilize the soft phonon and thus suppress the ferroelectric phase transition [1].

Pure  $\text{KNbO}_3$ , on the other hand, undergoes with decreasing temperature a series of successive phase transitions from a paraelectric cubic phase into a ferroelectric tetragonal phase, from the ferroelectric tetragonal phase into an orthorhombic ferroelectric phase, and finally from the orthorhombic ferroelectric phase into a rhombohedral ferroelectric phase. All these transitions are connected to a continuous phonon softening with decreasing temperature [2].

Solid solutions with niobium concentrations from 100% down to about 5% exhibit the same sequence of structural phase transitions as pure  $\text{KNbO}_3$  [3]. For lower niobium concentrations the situation is less clear. In the first published phase diagram, Rytz and

Scheel [4] indicate for niobium concentrations between 0.8 and 5% a single phase transition from the cubic to the rhombohedral phase. For low niobium concentrations (dilute KTN), it is still an open question whether KTN undergoes a true structural phase transition associated with a long-range ordering process or whether it freezes the dipolar and quadrupolar interactions and transforms into a polar glass without any symmetry change [5, 6]. Light scattering measurements of Lyons *et al* [7] on a sample with a niobium concentration of 0.9% reveal a relaxation which follows a Vogel–Fulcher law. This is evidence in favour of the formation of a glassy dipolar state. An extrapolation from the divergence of the relaxation time yields a transition temperature of 3 K. Inelastic neutron and light scattering measurements performed by Chou *et al* [8] in a solid solution with a niobium content of 1.2% show that the soft mode does not attain zero frequency but rather reaches a minimum of  $7 \text{ cm}^{-1}$  at 20 K. These authors attributed their findings to the transformation into a dipolar glass. This interpretation is in contrast to the results of a more recent Raman study by Toulouse *et al* [9]. They found a non-polar transverse optical mode ( $\text{TO}_3$ ) in the Raman spectrum and associated the appearance of this mode with a structural distortion. Recent dielectric and optical investigations of KTN crystals [10] with various niobium concentrations also indicate that the previously published phase diagram [4] has to be modified [10, 11].

Up to now all studies of KTN employing Raman [7, 9, 10], dielectric [5, 6], and neutron [8] spectroscopy focused on properties of phonons at the centre of the Brillouin zone. So far no attempt has been made to measure the phonon dispersion curves of KTN crystals with low niobium concentrations for finite wavevectors. In the following we present measurements of the lowest TO and transverse acoustic (TA) branches of the phonon dispersion curves in the (100) direction of the Brillouin zone by inelastic neutron scattering. We study the temperature dependence of the TA branch in two KTN crystals with niobium concentrations of 1.2 and 0.8%. Further we investigate the relations between the temperature dependences of the TO and TA branches and the phase transition and finally we calculate the correlation length in the soft phonon mode and compare the results with those in pure  $\text{KTaO}_3$ . A short summary of some results has been published elsewhere [12].

The paper is organized as follows. In section 2 we present the experimental results. Section 3 is devoted to the calculation of phonon frequencies and eigenvectors. The results are discussed in section 4. The final section is devoted to the conclusions.

## 2. Experimental details

### 2.1. Sample characterization and experimental set-up

We investigate two KTN samples with Nb concentrations of 0.8 and 1.2% and volumes of 3.5 and 1.5  $\text{mm}^3$ , respectively. Both samples have been grown from the melt by a slow-cooling method [4]. They show cubic (100) faces. The mosaic spreads of both samples have been checked by  $\gamma$ -ray diffraction. The first sample (0.8% Nb) has a mosaic width of  $20'$  whereas the second sample (1.2% Nb) shows a width of about  $40'$ .

The inelastic neutron scattering measurements were carried out on the spectrometer IN 2 at the ILL in Grenoble and on the spectrometer D 43 at CEA in Saclay, successively. The study of both samples concentrated on the temperature dependence of the TA and the lowest TO branch in the (001) direction in the temperature range between 300 and 4.2 K. Almost all measurements were carried out in the [220] Brillouin zone. Pyrolytic graphite was used as monochromator and analyser. All collimations were  $40'$ . Constant-energy scans were used for the steep parts of the dispersion curves. The other parts were measured by constant- $Q$

scans. Most measurements were made with an incident wavevector of  $k_i = 2.662 \text{ \AA}^{-1}$  and a graphite filter placed after the monochromator. A few additional scans were made at  $k_i = 3.1 \text{ \AA}^{-1}$ . In order to determine all three elastic constants supplementary scans of the low-frequency LA and TA phonons in the main symmetry directions were performed.

The Curie temperatures,  $T_C$ , have been determined from the step in the temperature dependence of the elastic constants. The ultrasound data [13] yield  $T_C = 0 \text{ K}$  for the first and  $T_C = 17.6 \text{ K}$  for the second sample with niobium concentrations of 0.8 and 1.2%, respectively. Thus the phase transition in the first sample is suppressed by quantum fluctuations. However, it should be pointed out that the phase diagram [4] at concentrations close to the critical niobium concentration of 0.8% exhibits a very steep increase of  $T_C$  with increasing niobium concentration. Since we cannot exclude a small concentration gradient across the sample, we have to admit that the exact niobium concentration of the first sample may vary between 0.8 and 0.9% [13].

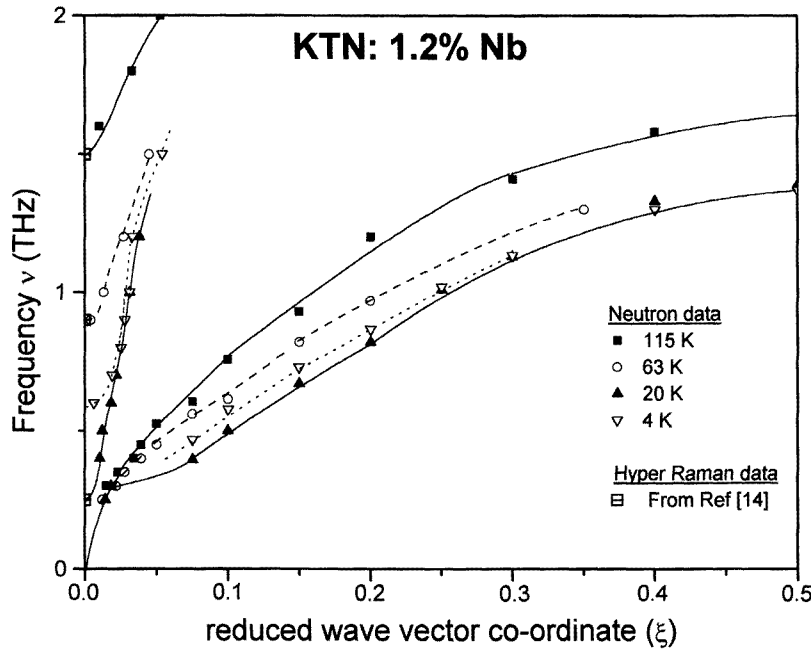


**Figure 1.** Phonon dispersion curves of the two lowest transverse branches in the (001) direction of KTN with a niobium content of 1.2 at.%. The experimental data at various temperatures are represented by symbols. Lines are drawn through the data points to guide the eye.

## 2.2. Phonon dispersion curves of KTN with a niobium concentration of 1.2%

We first focus on KTN with a niobium concentration of 1.2%. Figure 1 displays the measured phonon dispersion curves in the (001) direction as obtained from constant-frequency and constant-wavevector scans at temperatures of 115, 63, 20, and 4 K, respectively. We find a pronounced temperature dependence of TA phonons in the (001) direction for wavevector components larger than  $\xi = q(a/2\pi) = 0.04$ , where  $q$  is the phonon wavevector,  $a$  is the lattice constant, and  $\pi/a$  is the zone boundary. The TO branch shows quite a different behaviour. The frequencies of the lowest TO branch also vary

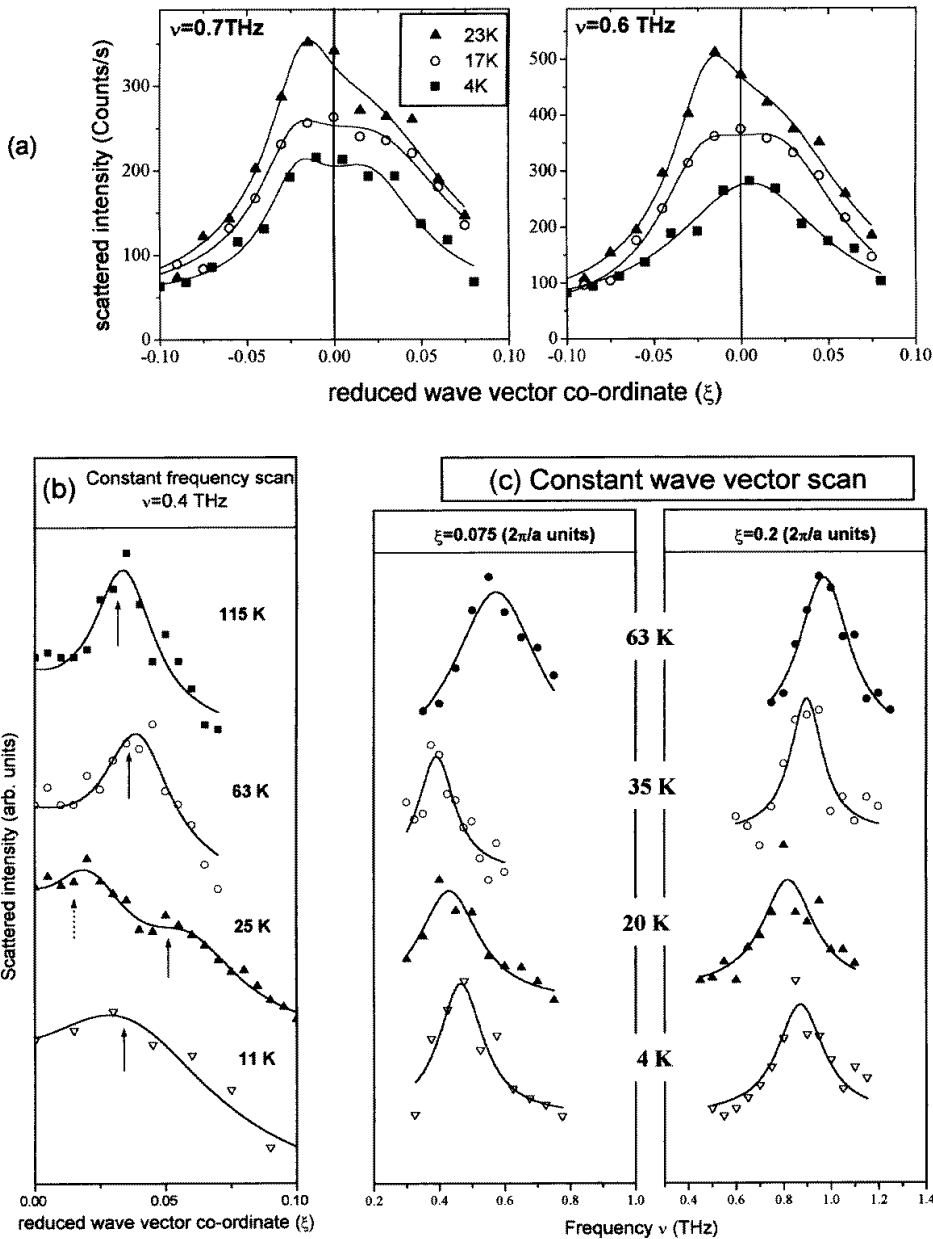
strongly with temperature but this variation takes place only for very small wave vectors ( $\xi < 0.1 \times 2\pi/a$ ). This feature of the TO branch is a familiar characteristic of crystals undergoing a ferrodistorive phase transition whereas the behaviour of the TA branch is quite different and less well known.

Of particular interest is the temperature dependence of the TO and TA phonons for small reduced wavevectors ( $\xi \leq 0.02$ ) at temperatures close to the phase transition which is expected to occur at about 20 K. In the following we analyse the scattering intensity at various temperatures. We first consider constant-energy scans through the TO branch in the (001) direction. The data reported in figure 2(a), for  $\nu = 0.7$  and 0.6 THz at  $T = 23, 17,$  and 4 K were recorded in the [220] Brillouin zones as a function of wavevector along the [00 $\xi$ ] direction with an incident wavevector  $k_i$  of  $2.662 \text{ \AA}^{-1}$ .

We now take a closer look at figure 2(a). At  $T = 23$  K, the curve recorded for  $\nu = 0.7$  THz exhibits two distinct maxima. This reveals that the scan clearly cuts the TO branch at relatively large wave vectors. At  $T = 4$  K, on the other hand, only one broad maximum centred around  $\xi = 0$  is observed. This indicates that the resolution ellipsoid marginally hits the frequency surface of the TO branch. The shape of the scan at  $T = 17$  K corresponds to an intermediate case. The results of the three scans indicate that the lowest and the highest zone centre frequencies of the TO branch occur at  $T = 23$  and 4 K, respectively. This finding is confirmed by data recorded for  $\nu = 0.6$  THz. The peaks at 23 K and at 17 K of the  $\nu = 0.6$  THz scans appear at smaller reduced wavevector coordinates  $\xi$  than those of the  $\nu = 0.7$  THz scans. The fact that the peak at 4 K is narrower for the  $\nu = 0.6$  THz scans than for the  $\nu = 0.7$  THz scans shows that the wavevector of the phonon is very close to  $\xi = 0$ . Thus the increase in frequency of the TO phonon below about 21 K indicates a phase transition at that temperature.

In the vicinity of the transition temperature, the analysis of the neutron data recorded at low frequency and small wavevector becomes rather difficult due to contamination by elastic scattering from the Bragg reflections and the simultaneous presence of TO and TA branches in the same frequency range (cf. figure 1). Figure 2(b) shows a series of constant-energy scans at 0.4 THz along the (001) direction at various temperatures. At 115 K and at 63 K a single, well defined peak arises from the scattering by the TA phonon. It should be noted in passing that the reduced wavevector component  $\xi_{max}$  of the peak increases with decreasing temperature (cf. Figure 1). The spectrum at 25 K shows two broad bands, the first being due to a TO phonon at  $\xi = 0.02$  and the second arising from the TA phonon with a reduced wavevector coordinate  $\xi = 0.05$ . In this situation where TA and TO phonon peaks are very close to each other, resolution calculations have been a valuable tool for the precise determination of phonon frequencies and wavevectors [12]. The spectrum at  $T = 11$  K exhibits a single peak. We attribute this peak to the scattering by a TA phonon with a wavevector smaller than that of the corresponding peak in the spectrum at 25 K. This shift in wavevector clearly indicates a hardening of the TA branch for temperatures below 20 K. This hardening correlates with an increase in the frequencies of the TO branch at and close to the origin of the Brillouin zone (BZ). We have previously shown [12] that the temperature dependences of TO and TA branches are closely correlated when the temperature decreases towards  $T_C$ . The softening of the TO phonon at the zone centre goes hand in hand with the frequency decrease of the TA phonon in the (100) direction. We show below that the analysis of the behaviour of the TA phonons can provide more useful information about the structural phase transition than the analysis of the zone centre TO phonon, which is more difficult to measure by inelastic neutron scattering.

Scattered neutron intensities recorded for constant reduced wave vector components  $\xi = 0.075$  and 0.2 along the (001) direction are reported in figure 2(c) for various

**KTN: 1.2% Nb**

**Figure 2.** Typical neutron groups in the  $(00\xi)$  direction of KTN with a niobium content of 1.2 at.%. (a) Constant-energy scans of transverse modes close to  $T_C$  at  $\nu = 0.7$  and 0.6 THz. Note the different shapes of the two scans at 4 K. The lineshapes at 4 K show clearly that the TO branch remounts below  $T_C$ . (b) Constant-energy scans of transverse modes at  $\nu = 0.4$  THz for various temperatures. The spectra are deconvoluted with the resolution function. The positions of the TA modes are indicated by solid arrows. The scattering spectra exhibit close to  $T_C$  a TO mode (dashed arrow) in addition to the TA mode (solid arrow). (c) Constant-wavevector scans of the transverse modes at  $\xi = 0.075$  and  $0.2$  ( $2\pi/a$  units) for various temperatures. Both series show a minimum in the TA frequencies at  $T_C$ .

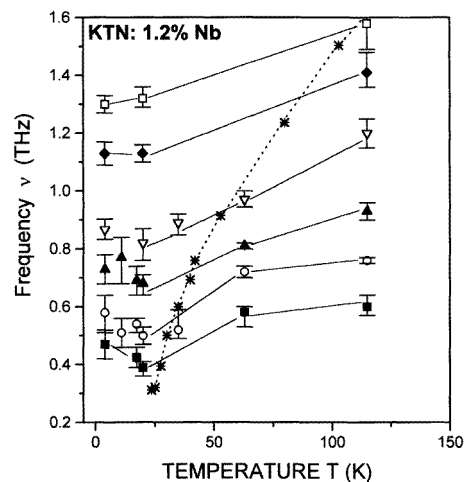


**Figure 3.** The temperature dependence of the TA phonon in the  $(00\xi)$  direction of KTN with a niobium content of 1.2 at.% for various reduced wavevector components  $\xi$  (■,  $\xi = 0.075$ ; ○,  $\xi = 0.1$ ; ▲,  $\xi = 0.15$ ; ▽,  $\xi = 0.2$ ; ◆,  $\xi = 0.3$ ; □,  $\xi = 0.4$ ). Typical error bars are indicated. For each  $\xi$ , the frequency exhibits a minimum at  $T_C$ . The frequency (\*) of the soft mode at the centre of the zone as obtained by hyper-Raman scattering [14] is reported for comparison.

temperatures. For both wave vectors the frequency  $\nu_{max}$  of the TA peak has the smallest value at  $T = 20$  K and then slightly increases with decreasing temperature. Figure 3 shows the temperature dependence of the frequencies of the TA phonons for various wavevectors along the  $(001)$  direction. The TA phonons undergo a large softening as the temperature approaches  $T_C$  from above. Below  $T_C$ , the TA modes start to reharden with further decreasing temperature. For comparison, the temperature dependence of the TO phonon at the zone centre as derived from hyper-Raman data [14] is also reported in figure 3. Since the available data are limited to temperatures above  $T = 20$  K, we only see the pronounced softening above the phase transition but not the rehardening below. It should be re-emphasized here that the pronounced temperature dependence of the TA frequency is observed for all wave vectors in the  $(001)$  direction with reduced wavevectors larger than 0.04 whereas the temperature dependence of the lowest TO branch is strongest at the zone centre and decreases rapidly with increasing wavevector.

In summarizing our inelastic neutron scattering results for KTN with a niobium concentration of 1.2% we find (i) a pronounced temperature dependence not only for the lowest TO phonon at the centre of the BZ but also for TA phonons along the  $(001)$  direction with reduced wave vector components larger than 0.04, (ii) a softening of TA phonons when the phase transition is approached *either* from above or from below, and (iii) a transition temperature of  $T = 20$  K, in agreement with the value derived from the SHG experiments on the same sample [14].

### 2.3. Phonon dispersion curves of KTN with a niobium concentration of 0.8%

We now focus on the inelastic neutron scattering data for KTN with a niobium concentration of 0.8%. First we consider again the lowest TO modes in the  $(001)$  direction. Figure 4(a) displays constant-frequency scans at  $\nu = 0.7$ , 0.6, and 0.5 THz for  $T = 12$  and 4 K. The spectrum for  $\nu = 0.7$  THz exhibits for both temperatures pronounced peaks which become at  $\nu = 0.6$  THz broad structures and disappear finally at  $\nu = 0.5$  THz completely leaving a single broad peak behind which is centred at the zone centre. The spectra for scans at different temperatures also show important differences. A characteristic shift is for example observed in the spectra for  $\nu = 0.7$  and 0.6 THz. In both spectra  $\xi_{max}$  is closer to zero for  $T = 4$  K than for  $T = 12$  K. This indicates that the TO branch for  $T = 12$  K is lower than

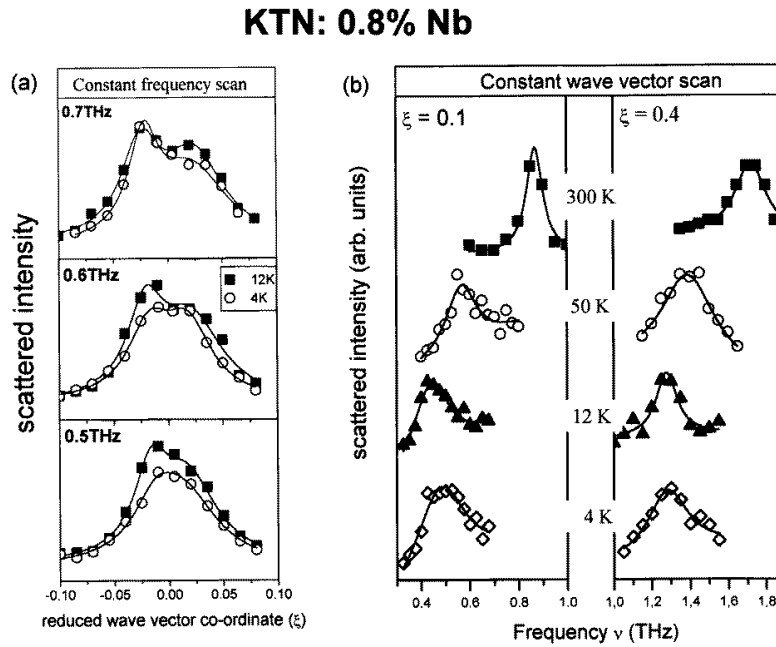


**Figure 4.** Typical neutron groups in the  $(00\xi)$  direction of KTN with a niobium content of 0.8 at.%. (a) Constant-energy scans of transverse modes at  $\nu = 0.7, 0.6,$  and  $0.5$  THz for  $T = 12$  and  $4$  K. (b) Constant-wavevector scans of the transverse modes at  $\xi = 0.1$  and  $0.4$  ( $2\pi/a$  units) for various temperatures. Note that the temperature dependence of the TA phonons exhibits a minimum at  $T = 12$  K.

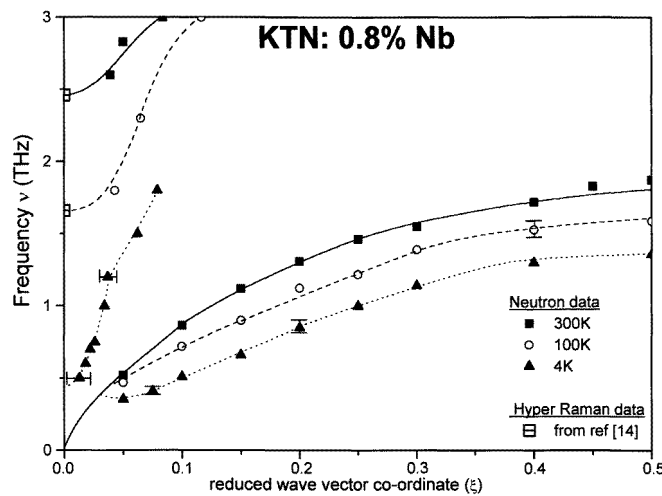


**Figure 5.** Phonon dispersion curves of the two lowest transverse branches in the  $(001)$  direction of KTN with a niobium content of 0.8 at.%. The experimental data at various temperatures are represented by symbols. Lines are drawn through the data points to guide the eye.

that for  $T = 4$  K. Since we have already shown that temperature dependences of the TO and the TA branches are related in the case of a niobium concentration of 1.2% we now



proceed to the investigation of the TA phonons in the (001) direction. Figure 4(b) shows two characteristic constant- $Q$  scans at  $\xi = 0.1$  and at  $\xi = 0.4$ . We clearly observe that the frequency  $\nu_{max}$  of the maximum of the scattered intensity decreases with decreasing temperature in the range from 300 to 12 K. Below 12 K, the frequency of the TA phonon starts however to increase slightly with decreasing temperature in the range from 12 to 4 K. Figure 5 displays the dispersion of the lowest TO and the TA branch in the (001) direction at 300, 100, and 4 K. Here again the pronounced temperature dependence of the TA branch extends throughout most of the (001) direction. The temperature dependence of various TA phonon frequencies is illustrated in figure 6. We find that the phonons in KTN with niobium concentrations of 1.2% and of 0.8% show in fact a very similar temperature dependence which occurs however on different temperature scales. The TA phonons first soften with decreasing temperature before they start to harden again. For each TA phonon, the minimum frequency is reached at 12 K. We thus conclude in analogy with the case for a niobium concentration of 1.2% that this temperature could be considered as the phase transition temperature for a niobium concentration of 0.8%. We finally point out that the softening of the TA phonons is again much smaller than that of the lowest TO phonon at the zone centre as derived from hyper-Raman data [14].

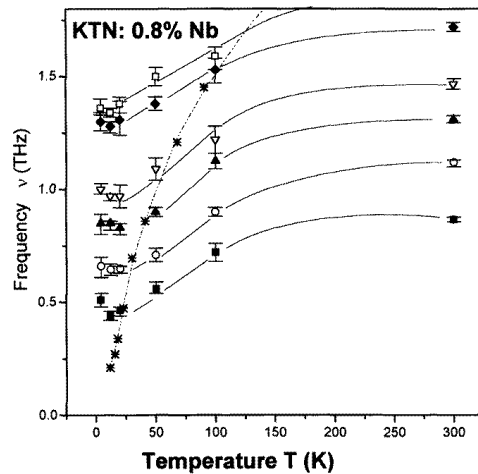


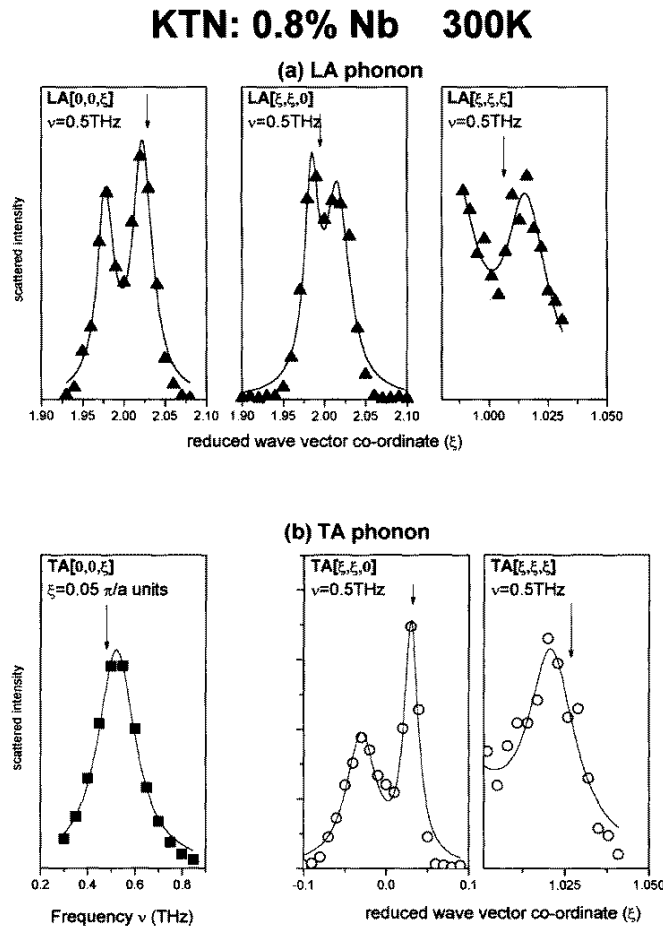
**Figure 6.** The temperature dependence of the TA phonon in the  $(00\xi)$  direction of KTN with a niobium content of 0.8 at.% for various reduced wavevector components  $\xi$  (■,  $\xi = 0.10$ ; ○,  $\xi = 0.15$ ; ▲,  $\xi = 0.20$ ; ▽,  $\xi = 0.25$ ; ◆,  $\xi = 0.40$ ; □,  $\xi = 0.50$ ). Typical error bars are indicated. For each  $\xi$ , the frequency exhibits a minimum at  $T_C$ . The frequency (\*) of the soft mode at the centre of the zone as obtained by hyper-Raman scattering [14] is reported for comparison.

The above-outlined indications for a phase transition in KTN with a niobium concentration of 0.8% are significant but not very pronounced. They are not confirmed either by ultrasonic [13] or by SHG [14] measurements. Hyper-Raman scattering measurements [14] exhibit a salient softening of the zone centre phonon as the temperature goes down to 11.5 K. At this temperature the TO frequency is about 0.25 THz. Unfortunately it is not possible to follow the TO mode below 11 K because of resolution problems.

The exact determination of the niobium concentration of the KTN samples used in various experimental studies is decisive for any comparison of results obtained with different techniques. Considering our actual knowledge of the samples used in the present studies, we conclude that a phase transition occurs at 12 K in KTN with a niobium concentration of  $0.008 \pm 0.0005$ .

**Table 1.** The relation between the slope of the acoustic phonons and the elastic constants.

Direction	LA	TA
[100]	$C_{11}$	$C_{44}$
[110]	$\frac{1}{2}(C_{11} + C_{12} + 2C_{44})$	$\frac{1}{2}(C_{11} - C_{12})$
[111]	$\frac{1}{3}(C_{11} + 2C_{12} + 4C_{44})$	$\frac{1}{3}(C_{11} - C_{12} + C_{44})$

**Figure 7.** Inelastic neutron scattering spectra of various acoustic phonons in KTN with a niobium content of 0.8 at.%. The symbols represent the experimental data. Lines are drawn through the data points to guide the eye. The arrows indicate the positions at which the peaks would be expected from an extrapolation of ultrasound data [13, 15].

#### 2.4. Elastic constants

Elastic constants  $C_{11}$ ,  $C_{12}$ , and  $C_{44}$  can be deduced from the slope of the acoustic phonon dispersion in the long-wavelength limit. The relations between the elastic constants and the slopes of the different branches in various directions of the Brillouin zone are summarized in table 1. In order to compare the experimental data obtained by our neutron scattering

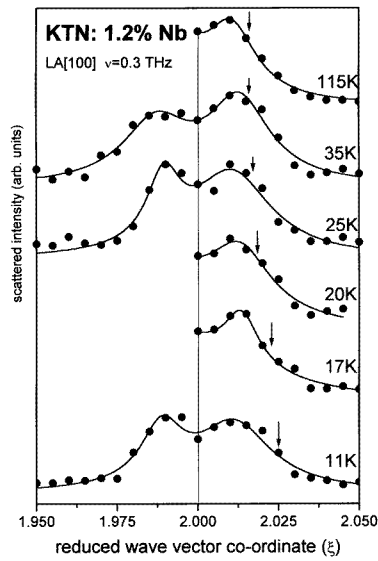


**Figure 8.** A constant-energy scan at  $\nu = 0.3$  THz of the LA mode in the (001) direction of KTN with a niobium content of 1.2 at.% for various temperatures. The peak position is nearly temperature independent whereas the position extrapolated from the ultrasound elastic constant  $C_{11}$  [13] (arrows) shows a rather pronounced temperature dependence.

measurements with those obtained by ultrasonic techniques we relate these with the reduced wavevector of the  $\nu = 0.5$  THz phonon calculated from elastic theory according to  $\xi = \nu a \sqrt{\rho/C}$  where  $C$  is the appropriate linear combination of elastic constants,  $\rho$  is the density, and  $a$  is the lattice constant. We present in figure 7 the neutron data recorded in KTN 0.8% at the constant energy  $\nu = 0.5$  THz for  $T = 300$  K. The results are indicated by arrows in figure 7. Since the ultrasonic measurements in KTN are confined to the determination of  $C_{11}$  [13] we take for  $C_{44}$  and  $C_{12}$  the data of  $\text{KTaO}_3$  [15]. The comparison yields a reasonably good agreement for all modes except the TA and LA phonons in the (111) direction.

It has been shown [13] that the elastic constant  $C_{11}$ , as derived from ultrasonic measurements, depends in the vicinity of the phase transition strongly on temperature. We therefore measured the long-wavelength LA phonons propagating along the  $[00\xi]$  direction as a function of temperature in KTN with a niobium concentration of 1.2%. The results for constant-energy scans at the lowest frequency we could attain (0.3 THz) are reported in figure 8. The results derived from ultrasonic measurements are again indicated by arrows. For all temperatures shown in figure 8, we observe a marked difference between the neutron scattering data and the data obtained from the ultrasound measurements. However, at 300 K the values coincide. With decreasing temperature the ultrasound values shift to larger reduced wavevectors due to a pronounced decrease in the ultrasound elastic constant whereas the neutron scattering peaks hardly change position. This marked difference is so large that it cannot be attributed to the poor accuracy of the neutron data. It is most likely that this discrepancy is due to the large difference between the frequency ranges probed by ultrasonic (10 MHz) and neutron scattering ( $10^6$  MHz) measurements. This may indicate that the lattice deformation associated with the cubic–rhombohedral transition affects only the acoustic phonons at very low frequencies and very large wavelength whereas the acoustic phonons in the THz range are practically decoupled from this process.

The elastic constant  $C_{44}$  as deduced in the long-wavelength limit from the slope of the TA branch in the  $[00\xi]$  direction is remarkably constant with temperature. This result is in perfect agreement with the ultrasound measurements of Barrett [15] on  $\text{KTaO}_3$ , who found that  $C_{44}$  in contrast to  $C_{11}$  is almost temperature independent. Our finding that for

very low wavevectors the TA branch is not affected by a coupling to the soft mode is thus confirmed by the ultrasound data. This result is expected from theoretical considerations. Since TO–TA coupling in the cubic phase is quadratic and not linear  $C_{44}$  should not vary with temperature.

### 3. Calculations

In order to analyse our results for KTN, we employ a shell model used by Perry *et al* [17] for the analysis of the phonon dispersion curves of pure  $\text{KTaO}_3$  and by us in a previous paper for the description of the lattice vibrations in KTN [16].

This model reproduces the experimental phonon dispersion curves obtained for  $\text{KTaO}_3$  [17, 18] as well as the softening of the TO phonon at the centre of the Brillouin zone with decreasing temperature [14], which arises from an increase of the electronic polarizability of the oxygen ion due to an on-site anharmonic coupling term of fourth order in the dipolar deformation of the electronic charge density of the oxygen ions.

In the following we focus on the question of whether or not such an anharmonic model is also able to explain the particular wavevector and temperature dependence of the TA phonons presented in the preceding sections. We show in particular that the anomaly in the dispersion of the TA branch is due to an exchange of the eigenvectors with the lowest TO branch. It should be mentioned in passing that an anomaly in the TA dispersion curve of an (incipient) ferroelectric was first detected in pure  $\text{KTaO}_3$  by Axe *et al* [18], who suggested a TO–TA coupling and a lattice instability caused by an acoustic mode.

The parameters of the model are given in table 2. These parameters are based on those determined for  $\text{KTaO}_3$  by a least-squares fit to the measured phonon dispersion curves in the main symmetry directions [17]. In order to account for the new data for KTN slight readjustments have been made. Nonetheless a unique set of parameters was maintained. These parameters define a model which describes the lattice vibrations of the KTN system for all niobium concentrations and all temperatures with a unique set of parameters of which none depends on the temperature and only one,  $k_{O-B}$ , (describing the nonlinear polarizability of the oxygen ions) on the niobium concentration. The solid solutions are treated in the virtual crystal approximation in which an effective mass  $M_B = M_{Ta}(1 - x) + xM_{Nb}$  is assigned to the B ions of  $\text{ABO}_3$ .

The results of the calculations for niobium concentrations of 0, 0.8, and 1.2% are compared to the experimental data for the lowest TO and TA branches along the cubic (00 $\xi$ ) axis in figure 9. The agreement between measured and calculated data for the TA branch is good for all concentrations at all temperatures. It should be pointed out that the model also reproduces the dispersion curves for crystals with much larger niobium concentrations of 37 [19] and 100% (the nominally pure  $\text{KNbO}_3$ ). The agreement between measured and calculated data for the TO branch is only satisfactory for pure  $\text{KTaO}_3$ . For niobium

**Table 2.** Shell model parameter values used in KTN.

Short-range interactions ( $e^2/2v$ units)							
$A_{K-O}$	$B_{K-O}$	$A_{B-O}$	$B_{B-O}$	$A_{O-O}$	$B_{O-O}$		
12.0	-0.21	359.0	-68.0	3.22	1.085		
Ionic and shell charges ( $e$ units)				Core-shell coupling ( $e^2/v$ units)			
$Z_K$	$Z_B$	$Y_K$	$Y_B$	$Y_O$	$k_K$	$k_B$	$k_{O-K}$
0.82	4.84	-0.419	7.83	-3.01	1000.0	1283.0	410.0

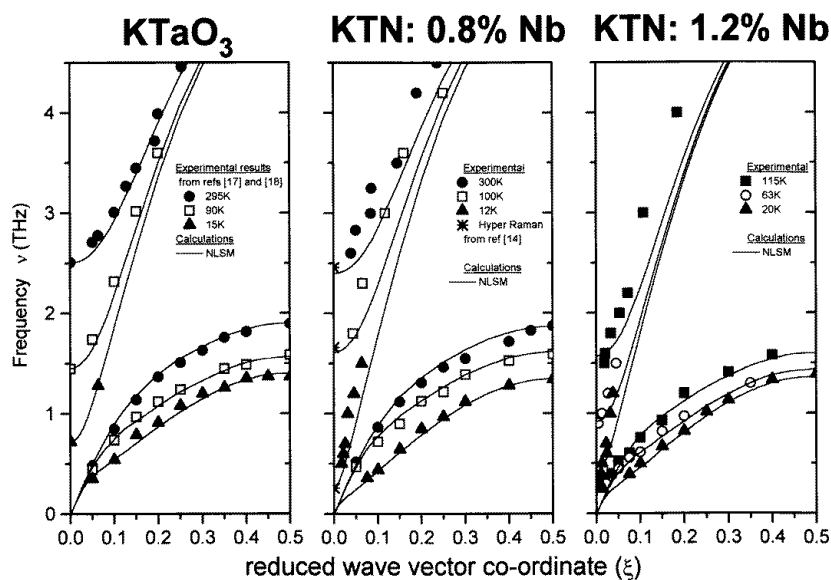


**Figure 9.** Measured (symbols) and calculated (lines) phonon dispersion curves of the two lowest transversal branches of KTN in the (001) direction at various temperatures and for various Nb contents (0, 0.8, 1.2 at,%).

concentrations of 0.8 and 1.2% measured and calculated frequencies deviate significantly for small wavevectors ( $\xi \leq 0.2$ ). The possible origin of these deviations is discussed in section 4.

The model calculations yield the dispersion not only of the phonon frequencies but also of the eigenvectors which are proportional to the displacements of the ions. In figure 10 we show the dispersion of the relative displacements for the lowest TO and the TA phonons in the (001) direction for the three niobium concentrations at various temperatures. The relative displacements are the real displacements of the ions apart from a common factor which cannot be determined for a linear system of equations. We focus first on the room-temperature results for  $\text{KTaO}_3$ . The highest branch conserves its TO character throughout the whole Brillouin zone whereas the lowest branch which has TA character for small wavevectors adopts TO character for wave vectors larger than  $\xi_c(\text{TA}) = 0.25$  since the oxygen ions start to vibrate in antiphase to the K and B ions. The niobium doped crystals show similar behaviour. Therefore we only plot the displacements of the O and the B ions since they are sufficient to decide the TO or TA character of the two lowest branches. Next we consider the temperature and concentration dependence of the reduced wavevector  $\xi_c$  at which the crossover from acoustic to optic character takes place. With decreasing temperature the reduced wavevector  $\xi_c$  at which the lowest branch loses its TA character shifts significantly to smaller wavevectors. As the transition temperature is approached the shift increases (cf. the curves for 12 K and 0.8% Nb or for 20 K and 1.2% Nb). Close to the transition temperature the upper branch exhibits TO character only for very small wavevectors and adopts an unexpected TA character in the main portion of the (001) direction. The crossover wavevector  $\xi_c(\text{TO})$  for the change in character for the upper branch is clearly different from  $\xi_c(\text{TA})$  of the lower branch. It also depends on the temperature and the niobium concentration. Figure 10 shows that close to the phase transition both branches

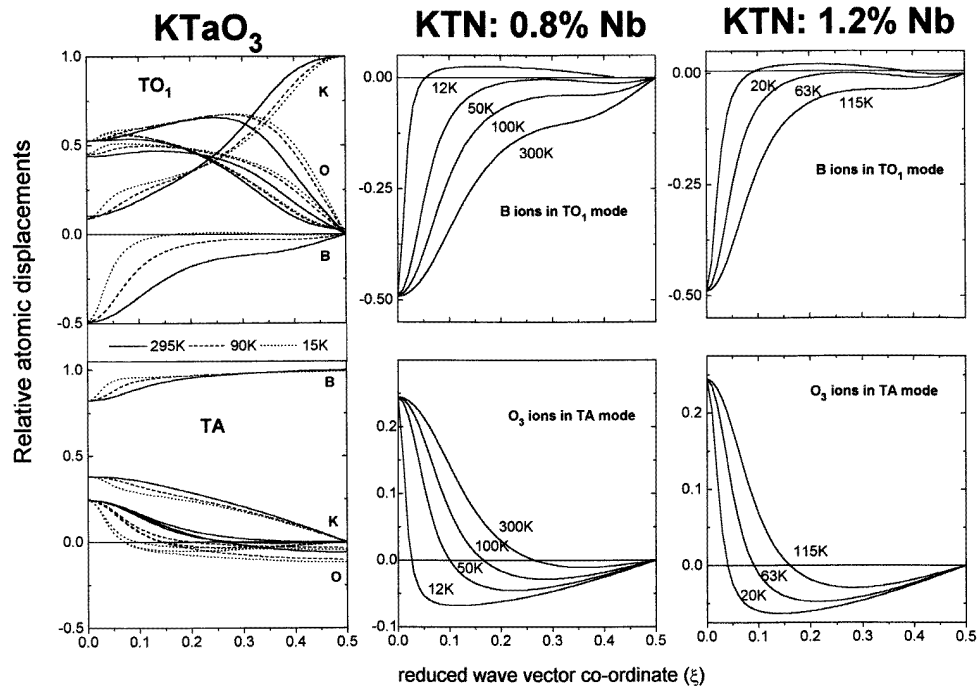


**Figure 10.** The temperature dependence of the relative displacements of the K, the B (Ta or Nb), and the O ions in the two lowest transverse modes along the (001) direction as calculated with the nonlinear shell model (NLSM) for pure and doped  $\text{KTaO}_3$ . For the assignment of an optic or an acoustic character to these modes it is sufficient to consider the displacements of the B ions in the upper branch and the O ions in the lower branch. The sign of these displacements determines the optic or acoustic character of the phonons.

assume their expected TA and TO character for very small wavevectors only. For larger wavevectors they change character. This explains very well the pronounced temperature dependence of the so-called TA branch which is detected in all crystals for  $\xi > 0.05$  (cf. figures 1 and 5). At very small wavevectors the lowest branch still has TA character. It is thus relatively independent of temperature. Likewise, the highest branch shows a significant temperature dependence for small wavevectors for which it always assumes TO character. In the vicinity of the phase transition, the amplitude of the B ion in the TO branch is large only for very small wavevectors.

#### 4. Discussion

A careful analysis of the lowest TO branch for small wavevectors shows that the discrepancy between the measured and the calculated phonon frequencies is an intrinsic problem of KTN which cannot be overcome by a simple readjustment of model parameters. A closer examination of the lowest TO branches in  $\text{KTaO}_3$  and in KTN (cf. figure 9) reveals a characteristic difference in the shape of the dispersion curves of the TO phonons whereas the TA branch exhibits a rather normal behaviour which can be attributed to the variation of  $T - T_C$ ,  $T_C$  being a function of the niobium concentration. For the lowest TO branch (cf. figure 9) the situation is quite different. We find in undoped  $\text{KTaO}_3$  at long wavelength

( $\xi < 0.2$ ) a relatively broad minimum which is well reproduced by the calculations and deepens with decreasing temperature.

In niobium doped crystals the dispersion of the lowest TO branch is much steeper and leads to a narrower minimum which cannot be very well reproduced by the model. With decreasing temperature the differences become more and more pronounced. We call this correlated narrowing and deepening with decreasing temperature a droplike behaviour. For the niobium concentration of 1.2% the droplike behaviour is even more prominent than for the lower concentration of 0.8%. This change in shape is a new phenomenon which has to be distinguished from the well known critical behaviour of the frequency of the lowest TO mode at the zone centre. The latter is related to the modulation of dielectric properties with temperature whereas the former points to a change of the correlation length of the soft mode with niobium concentration which cannot be taken into account in the frame work of a virtual crystal model. The effect of the substitution of tantalum ions by niobium ions on the frequency of the soft mode at a wavelength which is large compared to the size of the sample, however, can be satisfactorily accounted for by the effective core-shell constant  $k_{OB}$  at the oxygen site. Mean field theory, however, is unable to account for the fact that in dilute KTN crystals only a few unit cells contain niobium ions. Therefore the model is unable to describe how the soft phonons, which are strongly influenced by the niobium ions, propagate through the crystal which is essentially made of  $\text{KTaO}_3$  unit cells.

**Table 3.** Correlation lengths  $r_c$  as determined from the dispersion curves of the soft mode close to the centre of the Brillouin zone.  $a$  is the lattice parameter.

$\text{KTaO}_3$		KTN:Nb 0.8%		KTN:Nb 1.2%	
$T$ (K)	$r_c/a$	$T$ (K)	$r_c/a$	$T$ (K)	$r_c/a$
295	$\sim 1$	300	$\sim 1$	115	2.1
170	1.3	100	1.9	63	4.7
77	2.0	50	3.7	35	7.7
28	3.5	20	12	23	16.7
4	3.8	12	25	20	17.8

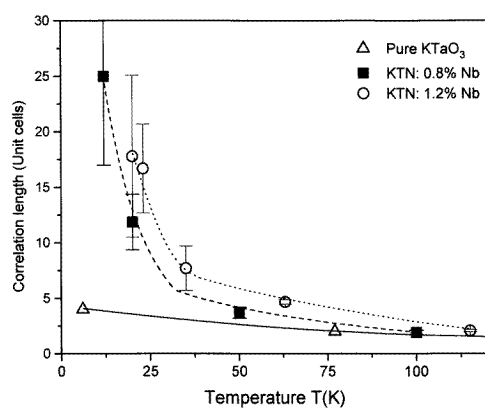


**Figure 11.** The temperature dependence of the correlation radius of the soft mode for KTN with Nb contents of 0, 0.8, and 1.2 at.% as calculated from the measured dispersion of the soft mode in the long-wavelength range of the (001) direction.

Finally we assign a correlation radius  $r_c$  to the parabolic dispersion of the optical branch by the well known equation

$$\omega_q^2 = \omega_0^2(1 + q^2 r_c^2)$$

where  $\omega_0$  is the frequency of the optical phonon at the zero wavevector and  $q$  is the wavevector. We determine the temperature dependence of the correlation length for three KTN crystals with niobium concentrations of 0, 0.8, and 1.2% from the dispersion of the TO branch. We have already pointed out above that our experimental data for the TO branch are not satisfactorily reproduced by lattice dynamical calculations. Therefore we use the experimental data in the small-wavevector range ( $qr_c < 1$ ) for the determination of  $r_c$ . In this wave vector range the upper mode corresponds to a pure TO motion and shows a quadratic dispersion. The calculated values of  $r_c$  are reported in table 3 for all three crystals. The temperature dependence of the correlation length is shown in figure 11. For the two doped samples, the correlation radius reaches its maximum value of about 20 lattice parameters at the transition temperature. This value is five times larger than the correlation length of pure  $\text{KTaO}_3$ . We thus conclude that the presence of defects enhances the correlation length of the TO mode. Since the correlation length is a measure for the size of polar distortions in the paraelectric phase, our results reinforce the assumption of the formation of polar clusters around niobium ions in the cubic phase. The values of  $r_c$  obtained from our measurements are in a good agreement with those obtained by Di Antonio *et al* [20] from Raman data for KTN with a niobium concentration of 1.2% as well as with those derived by Azzini *et al* [21] from SHG data for KTL with a lithium concentration of 1.6%.

## 5. Summary and conclusion

We have reported experimental data of the low-frequency TO and TA phonons in the (001) direction of two KTN crystals with niobium concentrations of 0.8 and 1.2% and analysed these data in the framework of an anharmonic shell model. We showed that not only the TO phonons at small wavevectors but also the TA phonon at large wave vectors exhibit characteristic shifts with temperature and niobium concentration.

We found that the temperature shift of the TA branch is due to an exchange of eigenvectors between the two lowest branches and that the crossover point shifts with decreasing temperature towards smaller wavevectors. We note that an analogous exchange of eigenvectors may cause the anomalies reported in the TA branch of  $\text{SrTiO}_3$  [22]. We would like to point out, however, that linear coupling terms vanish in cubic KTN whereas such terms may be present in  $\text{SrTiO}_3$  below the antiferrodistortive phase transition which occurs at 105 K.

We showed that both KTN crystals undergo a ferroelectric phase transition which is detected by the formation of a minimum in the frequency versus temperature curves for TA phonon with various wave vectors. The transition temperatures are  $T_C = 20$  K for KTN with 1.2% niobium defects and  $T_C = 12$  K for KTN with 0.8% niobium impurities.

The hardening of the soft phonon below  $T_C$  cannot be understood within a polar glass picture. Our findings show that the mechanism of the phase transition in dilute KTN is more complicated than the usual ferroelectric or the pure dipolar glass descriptions suggest.

The large displacements of the niobium ions in the soft mode affect neighbouring oxygen and tantalum ions in such a way that a long range dipolar correlation is established when the phase transition is approached. We showed that the soft mode still plays an important role for the phase transition and determines the size of the clusters although the phase transition in KTN cannot any longer be considered as strictly displacive. The size of the clusters is about 20 lattice parameters in dilute KTN crystals close to  $T_C$  and four lattice parameters in pure  $\text{KTaO}_3$  at 4 K.



## Acknowledgments

The authors express their gratitude to D Rytz for growing the crystals used in these experiments. The expert help of Drs B Hennion and N Lehner in the neutron experiments has been greatly appreciated.

## References

- [1] Wemple S H 1965 *Phys. Rev.* **137** A1575
- [2] Fontana M D, Métrat G, Servoin J L and Gervais F 1984 *J. Phys. C: Solid State Phys.* **16** 483
- [3] Triebwasser S 1959 *Phys. Rev.* **114** 63
- [4] Rytz D and Scheel H J 1982 *J. Cryst. Growth* **59** 468
- [5] Samara G A 1984 *Phys. Rev. Lett.* **53** 298
- [6] Kleemann W, Schäfer F J and Rytz D 1985 *Phys. Rev. Lett.* **54** 2038
- [7] Lyons K B, Fleury P A and Rytz D 1986 *Phys. Rev. Lett.* **57** 2207
- [8] Chou H, Shapiro S M, Lyons K B, Kjems J and Rytz D 1990 *Phys. Rev. B* **41** 7231
- [9] Toulouse J, Di Antonio P, Vugmeister B E, Wange X M and Knauss L A 1992 *Phys. Rev. Lett.* **68** 232
- [10] Bouziane E, Fontana M D and Kleemann W 1994 *J. Phys.: Condens. Matter* **6** 1965
- [11] Kleemann W 1993 *Int. J. Mod. Phys.* **7** 2469
- [12] Fontana M D, Kugel G, Foussadier L, Kress W and Rytz D 1993 *Europhys. Lett.* **23** 427
- [13] Rytz D, Châtelain A and Höchli U T 1983 *Phys. Rev. B* **27** 6830
- [14] Kugel G E, Vogt H, Kress W and Rytz D 1984 *Phys. Rev. B* **30** 985
- [15] Barrett H H 1968 *Phys. Lett.* **26A** 217
- [16] Kugel G E, Fontana M D and Kress W 1987 *Phys. Rev. B* **35** 813
- [17] Perry C H, Currat R, Buhay H, Migoni R L, Stirling W G and Axe J D 1989 *Phys. Rev. B* **39** 8666
- [18] Axe J D, Harada J and Shirane G 1970 *Phys. Rev. B* **1** 1227
- [19] Yelon W B, Cochran W, Shirane G and Linz A 1971 *Ferroelectrics* **2** 261
- [20] Di Antonio P, Vugmeister B E, Toulouse J and Boatner L A 1993 *Phys. Rev. B* **47** 10
- [21] Azzini G A, Banfi G P, Giulotto E and Hochli U T 1991 *Phys. Rev. B* **43** 7473
- [22] Vacher R, Pelous J, Hennion B, Coddens G, Courtens E and Müller K A 1992 *Europhys. Lett.* **17** 45